IJCRT.ORG ISSN : 2320-2882

INTERNATIONAL JOURNAL OF CREATIVE RESEARCH THOUGHTS (IJCRT)

An International Open Access, Peer-reviewed, Refereed Journal

SYNTHESIS AND CHARACTERIZATIONS OF CUO-ZNO NANO COMPOSITE BINARY OXIDE THICK FILMS AS H_2S GAS SENSOR

[1]Umesh J. Tupe, [2] M. S. Zambare, [3]A. V. Patil, [4]C.G. Dighavkar, [5]Amol S. Patil

[1]Department of Electronic Science, VADP's Arts, Science & Commerce College, Shirsondi, Tal – Malegaon, Dist-Nashik, Affiliated to SPPU, Pune, Maharashtra – 423208, India.

[2]Research Centre in Electronics, Department of Electronic Science, Fergusson College, Pune, (M.S.), Affiliated to Savitribai Phule Pune University, Pune, India.

[3]Department of Physics, MGV's, Arts, Science and Commerce College, Manmad, Dist. Nashik 423104, India

[4]Departmet of Physics, MGV's, Arts, Science and Commerce College, Surgana, Dist. Nashik 422211, India

[5]Department of Electronics, SSR College, Silvassa-396230, India

Abstract:

CuO and ZnO nanoparticles were synthesized using cost effective precipitation and green synthesis methods respectively. Synthesized nanoparticles were used to establish CuO-ZnO binary oxides thick films. Thick films have been developed by standard screen printing technique on a glass substrate. The structural characterizations of films were studied using FESEM, EDAX and XRD. The electrical characterization of thick films were studied using resistivity, activation energy and temperature coefficient of resistance (TCR). The XRD plots matched perfectly with JCPDS card number 80-1916 and 80-0074 for CuO and ZnO respectively and found that ZnO has hexagonal structure and CuO has monoclinic structure. Hydrogen sulphide gas sensing mechanisms of these films were investigated at various operating temperatures and PPM concentrations of gas. The 5% ZnO doped CuO binary oxide thick films shows maximum sensitivity of 78.8% sensitivity to 100 ppm of H_2S gas at operating different temperature 50^0 C. The films also showed a rapid response time of 8 seconds and recovery time of 20 seconds.

Keywords: *Synthesis, Nanoparticles, Binary oxide, Sensitivity, H_2S gas.*

1. Introduction

Because of the increased concentrations of poisonous gases in the environment due to industry, inorganic farming, cars, and other sources, the development of efficient gas sensors for the detection of harmful gases is critical. A gas sensor is a device that can tell us about the chemical composition of the air around it [1].Over 68 years ago, Brattain and Bardeen reported that gas absorption on the surface of a semiconductor can cause a change in the material's resistance. Since then, Seiyama et al 1962 and Taguchi 1970 have made persistent and effective efforts to use this change for gas detection [2, 3]. Metal oxides are one of them, and they are considered feasible materials for gas sensor applications due to their high stability, sensitivity, and ability to detect a wide range of target gases. Metal-oxide gas sensors have a number of drawbacks, including a long response time, low conductivity, a high operating temperature, and a slow recovery time. Gas sensors based on Metal Oxide Semiconductors have been utilized to monitor flammable and harmful gases in both residential and industrial environments. Because of their wide range of applications, low cost, reliability, small size, and low power consumption, gas sensors are in high demand [3, 4]. The two types of metal oxide semiconductors (MOS) are n-type and p-type. Electrons make up the majority of charge carriers in n-type MOSs, whereas holes make up the majority of charge carriers in p-type MOSs. MOS-based sensors work on the principle of resistance changes when exposed to the target gases or humidity. Oxidizing gases raise n-type semiconductor resistance while lowering p-type semiconductor resistance, whereas reducing gases do the opposite. Resistance decreases when p-type films are exposed to oxidising gases, but resistance increases when exposed to reducing gases. The resistance of n-type films increases when exposed to oxidising gases, while resistance decreases when exposed to reducing gases. When target gases combine with oxygen species, free electrons are produced [4-6]. Although p-type MOS has its own advantages, such as superior catalytic properties and lower humidity and operating temperature dependence [7, 8], N-type MOS has better sensitivity to target gases than p-type MOS. Traditional fabrication techniques have improved, allowing for the production of low-cost sensors with good response and dependability. Researchers wanted to create a highly sensitive gas sensor that could respond quickly and recover quickly. The detecting performance of MOS gas sensors is influenced by operating temperature, specific surface area, crystalline size, crystal structure, and resistivity quality. During the last few decades, extensive research has used doping methods to improve the characteristics of MOS. Doping and flaws have played a key role in enhancing material structural, electrical, optical, and mechanical properties over the years. Due to the deployment of sophisticated production and characterization technologies, we are mechanical properties by altering the fundamental structure at the nano-scale. Such research and discoveries are necessary to address technological, economic, and environmental challenges [9, 10].

2. Experimental work

2.1 Synthesis of copper oxide nanoparticles using precipitation method:

Cupric acetate [Cu (CH_3COO). H_2O] was used as a source of copper. Cupric acetate (7.9 gm) and NaOH pellet (5.4 gm) were dissolved separately into distill water (100 ml). The solution of cupric acetate and distill water stirred continuously at 80 ^oC for one hour using magnetic stirrer. Initially the cupric acetate greenish color and pH of solution is 5.29. Figure 1 (a) indicates the pH of cupric acetate and distills water solution. During the stirring NaOH solution mix drop wise in the cupric acetate solution still pH of solution reached at 11.20. Figure 1(b) indicates the pH of cupric acetate solution after added NaOH. After that the formation of obtained compound filtered using whatman filter paper 41 Figure 1(c). Using silica crucible the obtained compound was sintering at 400^oC for 2 hours. After that nanoparticles of CuO obtained shown in Figure 1 (d).

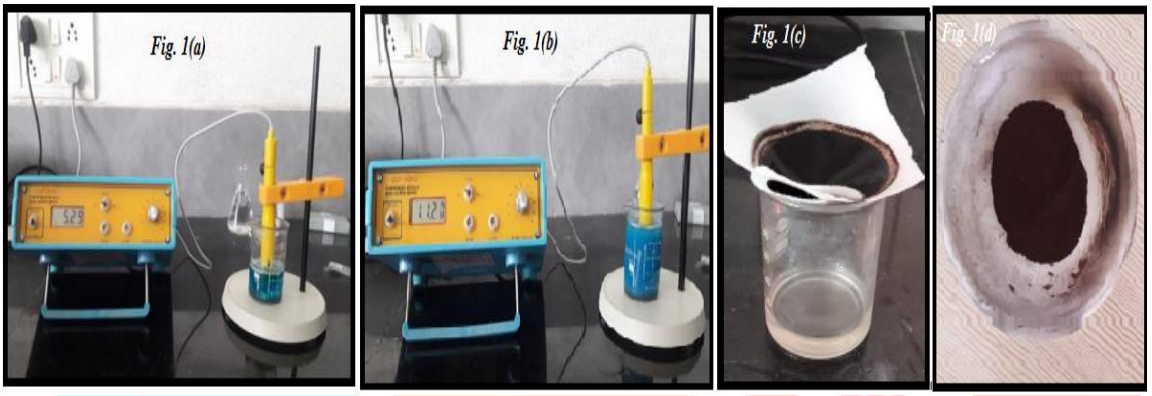

Figure 1 (a): The pH of cupric acetate and distills water solution, (b): The pH of cupric acetate solution after added NaOH, (c): Filter obtained compound using whatman filter paper 41 and (d): Obtained copper oxide nanoparticles after sintered at 400^oC.

2.2 Synthesis of ZnO nanoparticles using green synthesis method

The nanoparticles of zinc oxide synthesis by green synthesis method using zinc nitrate Zn ($NO_3O_2.6H_2O$). Zinc nitrate is a source of Zn. In this experiment 0.02M of Zinc nitrate hexa hydrate in 250 ml beaker and dissolved it into 50 ml distilled water, i.e. 5.94 gm of Zn ($NO_3O_2.6H_2O$) in 50 ml distilled water. During the addition of zinc nitrate in distilled water constant string is necessary after that aqueous leaf extract of corriandrum is introduces into above solution of zinc nitrate in the following particular set of addition of this extract into the solution. The obtained precipitate is dry at room temperature of 15-18 hrs then power of 240 pale white colored is dry on hot plate at 80- 90^oC for 5 hrs and after that pale white colored nano composites of ZnO is obtained. The flow chart of the experimental work performed for synthesis of ZnO nanoparticles using green synthesis method mention in Figure 2.

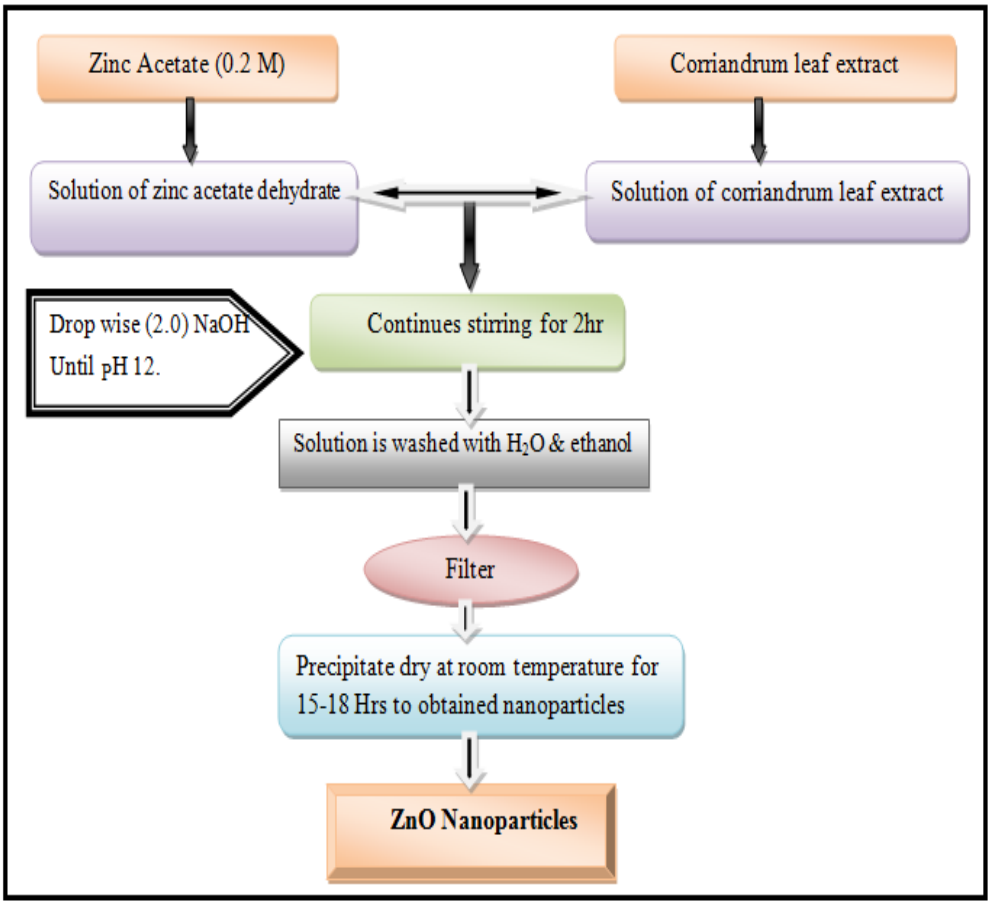

Figure 2: Synthesis of ZnO nanoparticles using green synthesis method

2.3 Preparation of pastes of additive and functional materials for thick films

Inorganic material 70% and organic material 30% were taken to prepare ZnO doped CuO binary oxide thick films. Inorganic material consists of synthesized nanoparticles of functional materials such as CuO. Organic part consists of ethyl cellulose (8%) and butyl carbitol acetate (92%). The ethyl cellulose as used as temporary binder and BCA used drop wise to prepare paste with a proper viscosity and Wt. % additive at different concentration (1%, 3% and 5%) were added in the functional base inorganic material for preparation of nanocomposites binary oxide thick films.

2.4 Thick film preparation method

In the current research study, 120 mesh nylon screens were used to develop thick film. A 1.25 cm x 2.50 cm rectangular window was developed using standard lithographic techniques on the screen. Paste or ink is an important part of thick film printing. The paste is evenly pressed to the top of the screen using mechanical drainage. The paste forms a layer on the surface of the substrate. Layer work is done by the components of the paste. The paste contains nano sized functional metal oxide material, ethyl cellulose and temporary binder likes BCA as a solvent. Using squeegee paste is put on glass substrate using screen printing setup. Ones films are prepared it kept in ambient condition for settle down. The films were exposed to infra-red radiation for approximately 30 min. The organic solvents were removed by this exposure. Ones material pasted on the substrate becomes stable films are ready to use for further process. The next phase involves the heat treatment of the prepared thick films. After firing approximately 350 ^{o}C into the muffle furnace, the film's fine material becomes a solid composite. This process is called firing. Figure 3 shows the steps for preparation of CuO-ZnO binary oxides thick films.

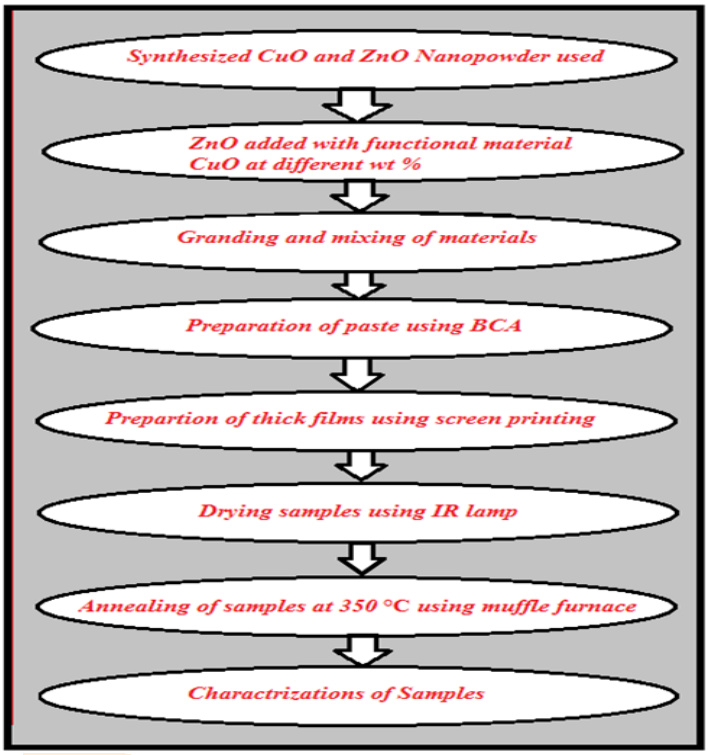

Figure 3: Steps for binary oxide thick film preparation.

2.5 Static system for study electrical and gas sensitivity

The D.C. resistance of the thick films was measured by using half bridge method as a function of temperature in home-built static measurement system as shown in Figure 4. The gas sensing study was also carried out using static gas system to sense H_2S gases. The binary oxide thick films were used as sensing component. The resistance of the sample was measured in an air atmosphere as well as in the presence of gas (at ppm level) of interest at different operating temperatures. The resistance (R_a) of the sample in air and (R_g) in gas atmosphere was measured by using half-bridge method [11-13].

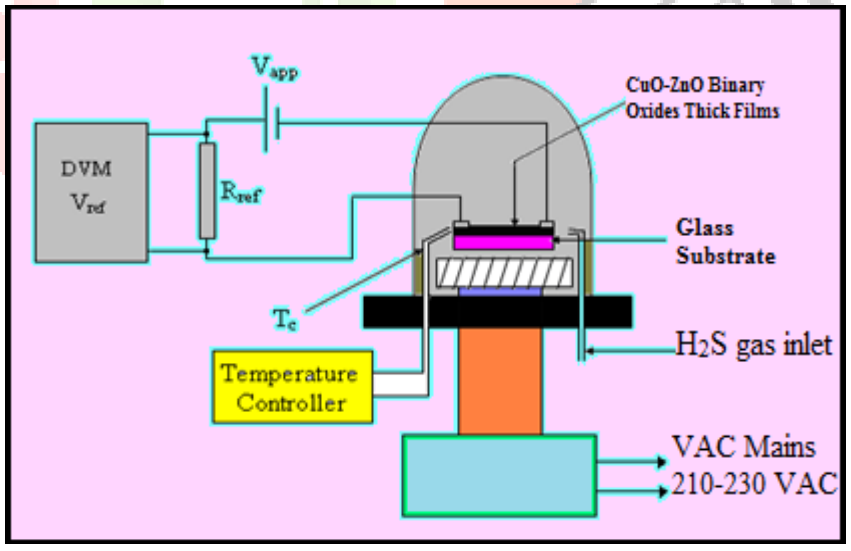

Figure 4: Schematic diagram of electrical and gas sensitivity static system.

2.6 Characterizations of CuO-ZnO binary oxides thick films

2.6.1 Electrical characterizations

2.6.1.1 Resistivity - The resistivity of the films was determined using following equation 1 [11],

$$\rho = \left(\frac{R \times b \times t}{l} \right) ohm - m \quad \text{..... (1)}$$

Where, t = thickness of the film sample, b = breadth of the thick film resistor in cm

2.6.1.2 Activation energy - The activation energy of thick film samples is calculated from Arrhenius plot using the equation 2 [11, 12],

$$R = R_o e^{-\Delta E/KT} \quad \text{..... (2)}$$

Where, R_o = the constant, ΔE = the activation energy of the electron transport in the conduction band (eV), K = Boltzman constant and T = Absolute temperature.

2.6.1.3 Temperature coefficient of resistance (TCR) - TCR was calculated by using the equation 3 [12],

$$TCR = \frac{1}{R_o}\left(\frac{\Delta R}{\Delta T} \right) \ /^{O} C \quad \text{..... (3)}$$

Where,

ΔR = change in resistance between temperature T_1 and T_2, ΔT = temperature difference between T_1 and T_2 and R_o = Initial resistance of the film sample.

2.6.2 Structural characterizations

The developed thick films were characterized by SEM, EDAX and XRD to study the surface morphology, elemental composition analysis and structural properties respectively. The thickness of the thick films was measured by using Taylor-Hobson (Taly-step UK) system. The thickness of the films was observed in the μm range [11].

2.6.2.1 Scanning Electron Microscopy (SEM) - It is convenient technique to study surface morphology. Scanning Electron Microscopy (SEM) {Model JOEL 6300 LA GERMANY} was utilized to characterize the surface morphology. The magnifications of all SEM images are taken at 5000X. Average particle size and diameter of nanoparticles were determined using Image-J software of SEM images of thick films. The specific surface area of thick films was calculated using BET method for spherical particles using the equation 4 [12].

$$S_w = \frac{6}{\rho d} \quad \text{……..} \quad (4)$$

2.6.2.2 Energy dispersive X-Ray analysis (EDAX) – It is powerful analytical technique which provides X-ray distribution images, line scans and point analysis of trace elements of micro-volumes. EDAX give ratio of expected compounds of the elements present in the film. First, the entire sample was scanned for SEM and then the elements were detected by EDAX. The elemental analysis was carried out carried out using energy dispersive X-ray spectrometer EDAX (JOEL-2300, Germany). The specimen image can be

obtained along with the elemental analysis of the selected area/features and distribution of selected elements.

2.6.2.3 X-ray diffraction (XRD) – XRD tool was used to determine the crystalline structure and preferential orientation of the crystallite material and also to determine the crystallite size. For thick films low angle XRD was used X-ray generator [Miniflex Model, Japan] Rigaku diffractometer (DMAX-500) was employed. The XRD gives d values which were used for identification of different phases and corresponding structure of the material present in the developed films. The experimental (observed from X-ray data) d values are compared with the standard data (JCPDS/ASTM data files). 2θ was carried out to examine the final compositions of the CuO-ZnO nano composite binary oxides thick films. The crystallite size (D) was estimated by Debye Scherer's formula equation 5 [11, 13].

$$D = \frac{0.9\lambda}{\beta Cos\theta} \qquad \text{..... (5)}$$

Where, β = Full angular width of diffraction peak at the at half maxima peak intensity.

λ =wavelength of X-radiation.

2.7 Investigate gas sensitivity

The H_2S gas response of thick films was studied in test assembly. The electrical resistances of nano composite binary oxide thick film in air (*R*a) and in the presence of H_2S gas (*Rg*) were measured to find the sensitivity (*S*) given by the equation,

$$S\% = \frac{Ra-Rg}{Ra} \times 100 \qquad \text{..... (6)}$$

Where, Ra is the resistances of the CuO-ZnO thick film in air and Rg is the resistances of the CuO-ZnO thick film in gas atmosphere.

3. Result and Discussion

3.1 Electrical Characterization

3.1.1 Resistivity

Resistance determines using home built characterization system. The DC resistance of films was determining by using half bridge method. Readings of temperature verses voltage were taken with the interval of 10°C temperature. The operating temperature range of thick films was 30°C to 350°C. The resistance of nano composite binary oxide thick films decreases with increase in temperature. This confirms the semiconductor behavior of ZnO: CuO nano composite binary oxide thick films by obeying $R= R_0e^{-\Delta E/KT}$ in the 30 °C to 350 °C temperature interval [11- 14].

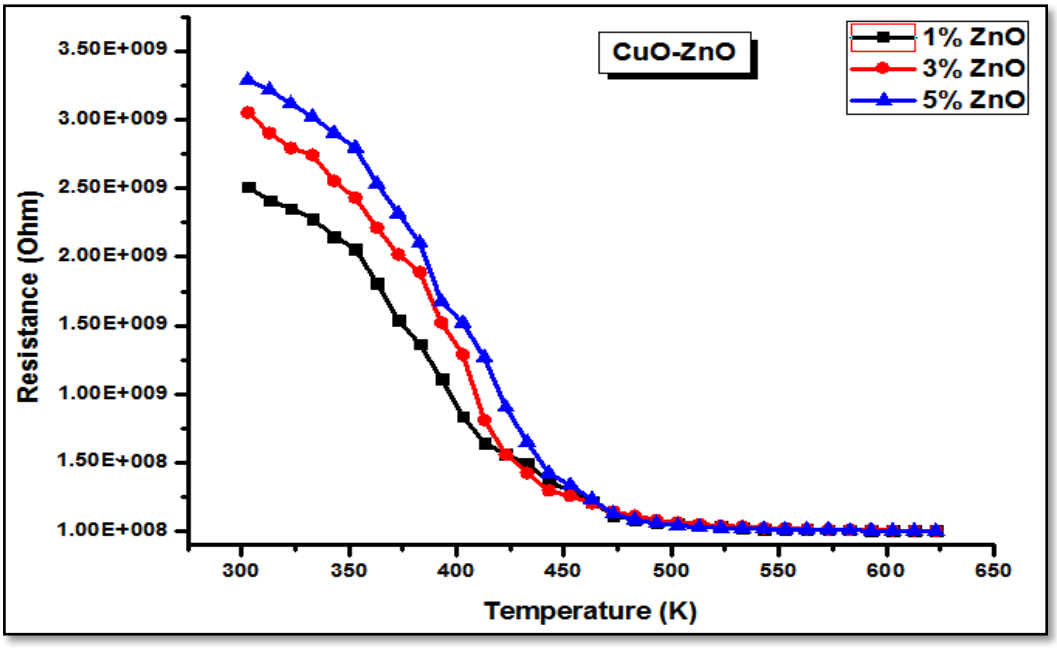

Figure 5 shows the change in resistance of 1 wt. %, 3 wt. %, and 5 wt. % additive (ZnO) added CuO thick film samples with respective change in temperature.

3.1.2 Activation Energy of ZnO: CuO nano composite binary oxide thick films

The activation energies of prepared ZnO: CuO nano composite binary oxide thick films in the low temperature and high temperature films were calculated using Arrhenius plot.

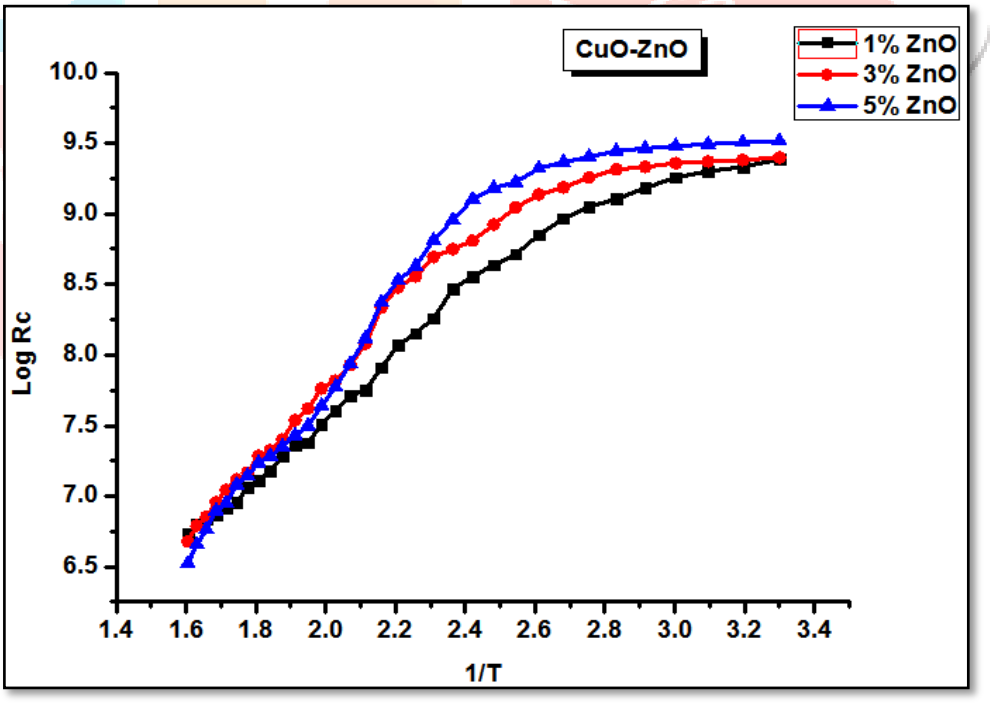

Figure 6 shows Arrhenius plot 1 wt. %, 3 wt. %, and 5 wt. % additive (ZnO) added CuO thick film samples.

In both cases i.e. heating and cooling cycles plot is found to be reversible and obeys the Arrhenius equation.

Table 1: Activation energy of ZnO: CuO thick film.

ZnO additive (wt. %) ZnO: CuO thick films	Activation energy (eV)	
	Low temperature region	High temperature region
1	0.3750	0.0619
3	0.6636	1.4211
5	0.7050	0.9456

The Activation energy for 1 wt. % for ZnO: CuO binary oxide thick film found 0.3750 eV and 0.0619 eV at low and at high temperature respectively. The Activation energy for 3 wt. % for ZnO: CuO binary oxide thick film found 0.6636 eV and 1.4211eV at low and at high temperature respectively. The Activation energy for 5 wt. % for ZnO: CuO binary oxide thick film found 0.7050 eV and 0.9456 eV at low and at high temperature respectively.

3.1.3 TCR of ZnO: CuO nano composite binary oxide thick films

The temperature coefficient of resistance (TCR) of ZnO: CuO nano composite binary oxide thick films are calculated by using equation 3.

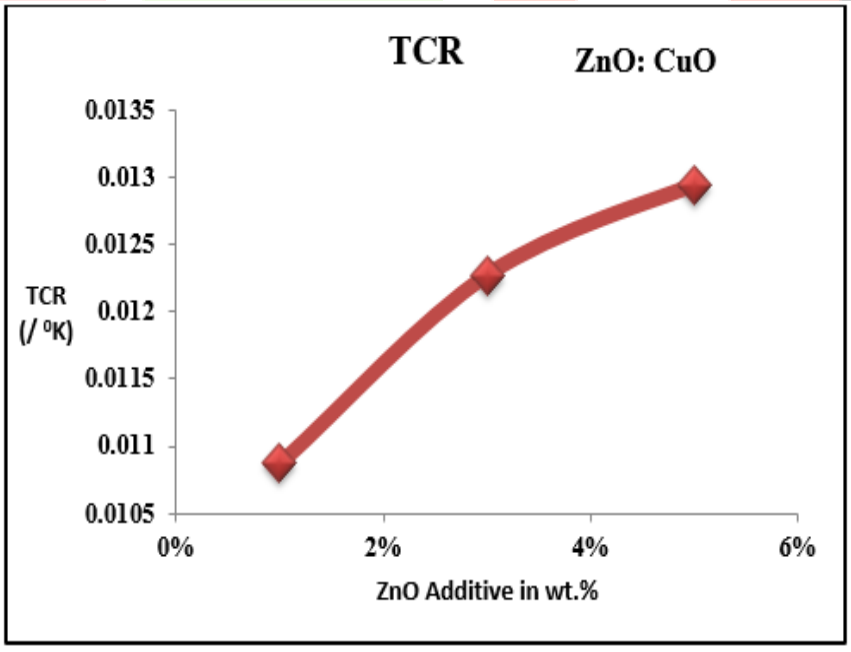

Figure 7: TCR of ZnO: CuO nano composite binary oxide thick films

Table 2: TCR of ZnO: CuO nano composite binary oxide thick films

ZnO additive (wt. %) ZnO: CuO thick films	**CR / ^{0} K**
1	-0.01087
3	-0.01227
5	-0.01294

Temperature coefficient of resistance is found negative to ZnO: CuO nano composite binary oxide thick films samples. The negative sign indicate the semiconductor behavior of the prepared thick films. High resistivity of thick film samples corresponds to a low TCR value [12].

Table 3: Electrical outcomes of ZnO: CuO nano composite binary oxide thick films

ZnO additive (wt. %) ZnO: CuO thick films	**Film Thickness (µm)**	**Resistivity(ρ) (Ω-m)**	**TCR (/°K)**	**Activation energy (eV)**	
				Low temperature region	High temperature region
1	24	30.01 X 10^4	-0.01087	0.7311	0.5999
3	26	40.30 X 10^4	-0.01227	0.7514	0.3825
5	25	41.25 X 10^4	-0.01294	1.2589	0.9543

Table-3 Present electrical characterization of ZnO: CuO nano composite binary oxide thick films sample. Table 3 indicates the different values of thickness and other electrical parameters for each of the ZnO: CuO nano composite binary oxide thick films sample.

3.2 Structural Characterization

3.2.1 SEM analysis of ZnO: CuO nano composite binary oxides thick films

Scanning electron microscopy (SEM) is one of the most popular and widely used techniques for the characterization of nanomaterial's and nanostructures. For the study of ZnO: CuO nano composite binary oxides thick films thick films thick film SEM magnification is 5000. The SEM images show the morphology of ZnO: CuO nano composite binary oxide thick films. wt. % of additive increases the change in surface morphology also found to be increasing in the SEM images. The particles grain size decreases with increases doping percentage of ZnO in the CuO. SEM results indicate the formation of particles with different shapes and sizes. The image shows, larger particles or grain agglomerates. SEM results also show particles have large porosity showing large numbers of voids. These voids are responsible for the adsorption of the gas molecules [15, 16].

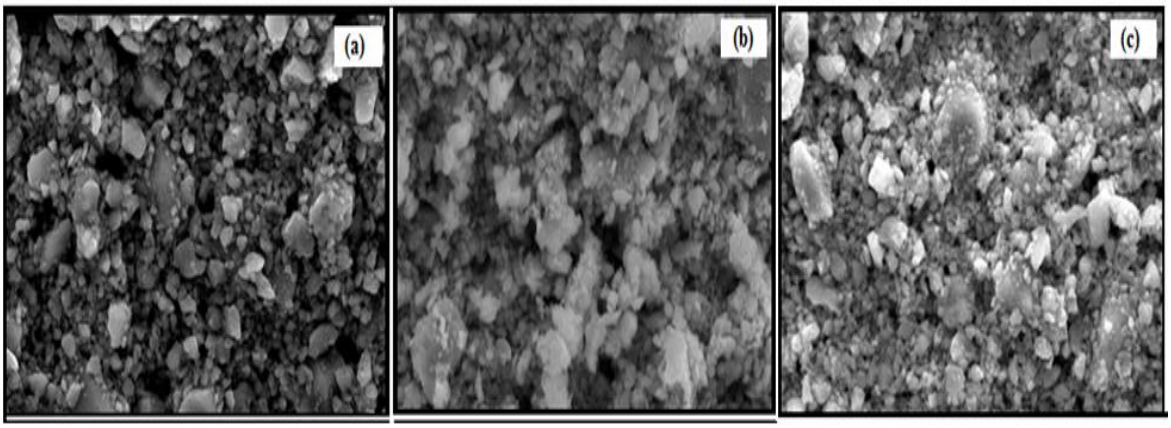

Figure 8 (a), (b) and (c) shows SEM images of 1 wt. %, 3 wt. %, and 5 wt. % additive (ZnO) added CuO thick film respectively.

The 2D images with high magnification were used to study surface morphology of these films. The specific surface area calculated by using SEM images. The diameter (*d*) of ZnO: CuO nanoparticles were measured by using Image J software. The rate of adsorption and desorption increases with large surface area of the films as well as nanoparticles of materials produced maximum chemisorption's. Using BET method, specific surface area of ZnO: CuO nano composite binary oxides thick films were calculated by equation 4 [12, 16].

Table 4: Specific surface area of ZnO: CuO nano composite binary oxide thick films.

ZnO additive wt%	Specific surface area in m^2/g
1%	1.3389
3%	2.2935
5%	2.7796

From above Table 4, it has been observed that the specific surface area of ZnO: CuO nano composite binary oxide thick films.

3.2.2 X-ray diffraction

The hkl parameters of CuO and ZnO match with JCPDS Card 80-1916 and 80-0074 respectively. Hence it clearly found that the structure of CuO is monoclinic and structure of ZnO is hexagonal for all percentage. Prominent peak of XRD found is at 38.71 which indicates [200] for 1wt. %, prominent peak of XRD found is at 35.63 which indicates [111] for 3wt. %, and prominent peak of XRD found is at 38.77 which indicates [111] for 5wt. %, Better crystallinity found because the maximum intensity of prominent peaks. The crystalline nature of the thick film material is confirmed by XRD. Average crystallite size was calculated from XRD pattern and using Debye-Scherrer equation 5 [12]. The crystallite size was found to be as 39 nm, 32 nm and 31 nm for 1 wt. %, 3 wt. %, and 5 wt. % respectively.

X-ray diffraction studies were conducted to understand the crystal structure and phase of ZnO: CuO nano composite binary oxide thick films. The CuKα radiation range is 20˚ to 80˚ for ZnO: CuO nano composite binary oxide samples. Following Figure 9 shows X-ray diffraction pattern obtained for 1 wt. %, 3 wt. %, and 5 wt. % ZnO: CuO thick films.

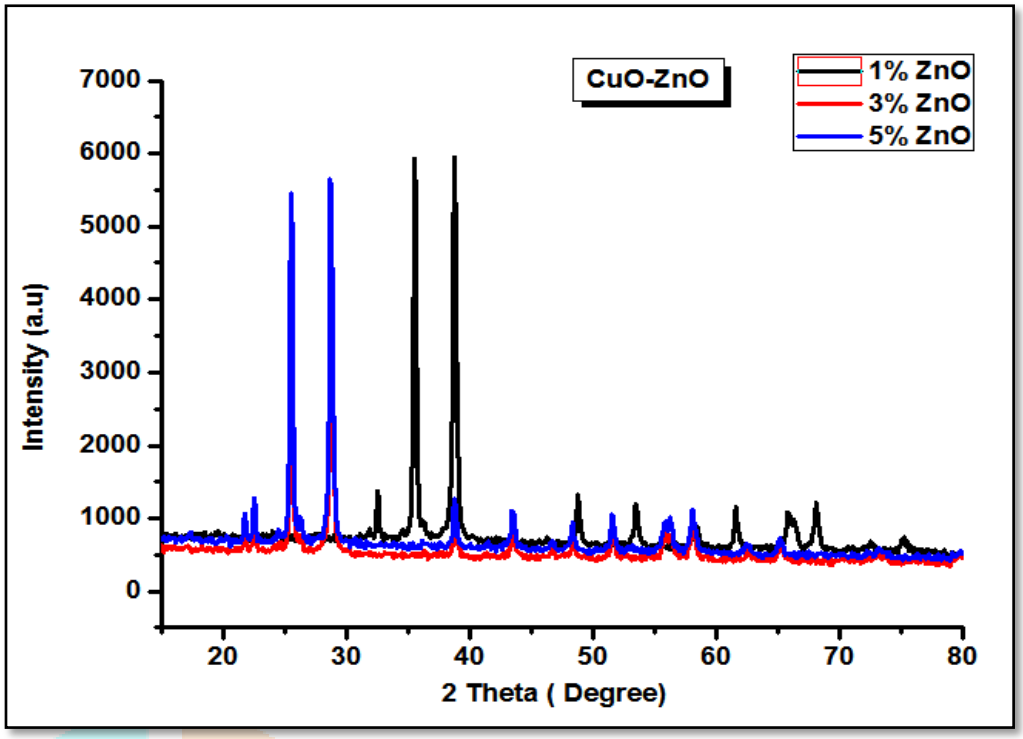

Figure 9**:** X-ray diffraction pattern of ZnO: CuO thick film samples

Table 5: Crystallite size for 1 wt. %, 3 wt. % and 5 wt. % concentration of ZnO added CuO thick film sensors

ZnO additive concentration (wt. %)	Average crystallite size (nm)
1	39
3	32
5	31

3.3. Gas sensing characterization

3.3.1 Study of H_2S gas sensing characterization of ZnO: CuO nano composite binary oxides thick films samples

The prepared ZnO: CuO nano composite binary oxides thick films samples were used as a H_2S gas sensor. Resistance of the film is measured in the form of voltage using half bridge method. This method is applied at different operating temperatures in H_2S gas atmosphere for ZnO: CuO nano composite binary oxides thick films samples. The H_2S gas was injected with different concentration level in ppm at normal atmospheric conditions.

3.3.2 Sensitivity on operating temperature with different concentration of H_2S gas in ppm.

The H_2S gas sensing behavior of ZnO: CuO thick films were studied by using home-built static measurement system. The ZnO: CuO nano composite binary oxides thick films sample resistance was measured by using half bride method with temperature in the H_2S gas atmosphere.

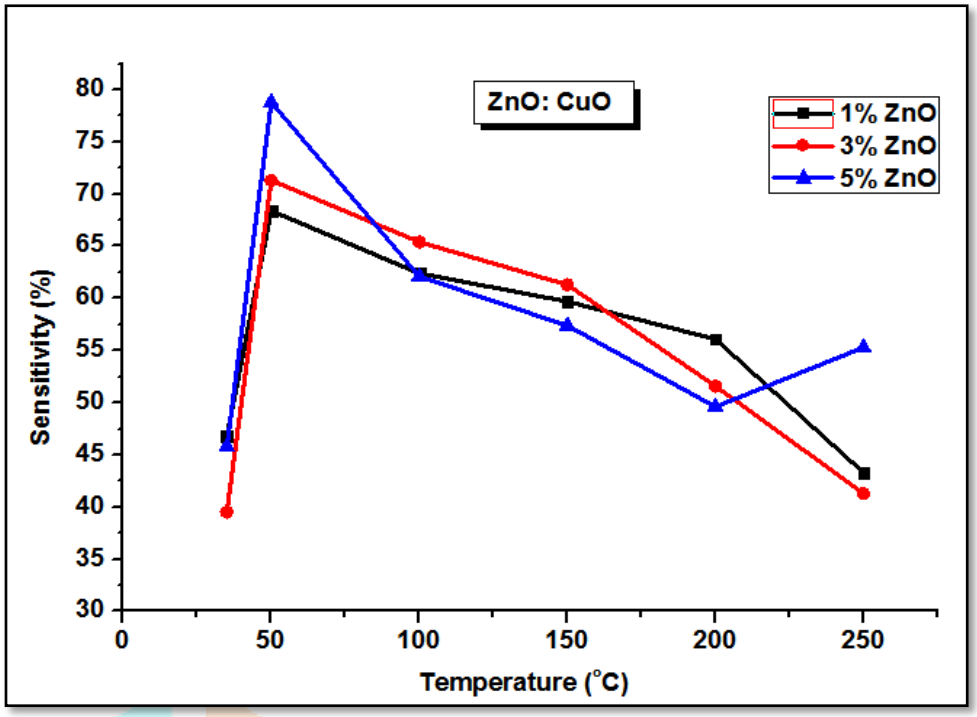

Figure 10: Sensitivity of ZnO: CuO nano composite binary oxides thick films sample

Time interval of operating temperature is 50°C during the measurement of gas response. For measurement of H_2S gas sensitivity the temperature range varied from room temperature (35°C) to 250°C. The gas sensitivity of the ZnO: CuO nano composite binary oxides thick films sample were calculated using equation 6. The concentration of H_2S gas in the current gas sensing study were taken in part per million (ppm). Here four concentrations 100 ppm, 200ppm, 500ppm and 1000 ppm of H_2S gas were used. Figure 10 shows the variation of % sensitivity for 1 wt. %, 3 wt. %, and 5 wt. % additive (ZnO) added CuO thick film samples. The 5% ZnO doped CuO binary oxide thick films shows maximum sensitivity of 78.8% sensitivity to 100 ppm of H_2S gas at operating different temperature 50^0 C.

3.3.3. Response time and recovery time of ZnO: CuO nano composite binary oxides thick films sample

The thick film sensor is kept at 50^0C optimum temperature. Then, H_2S gas is insert using syringe in the glass dome of the gas sensing system for measurement of response time.

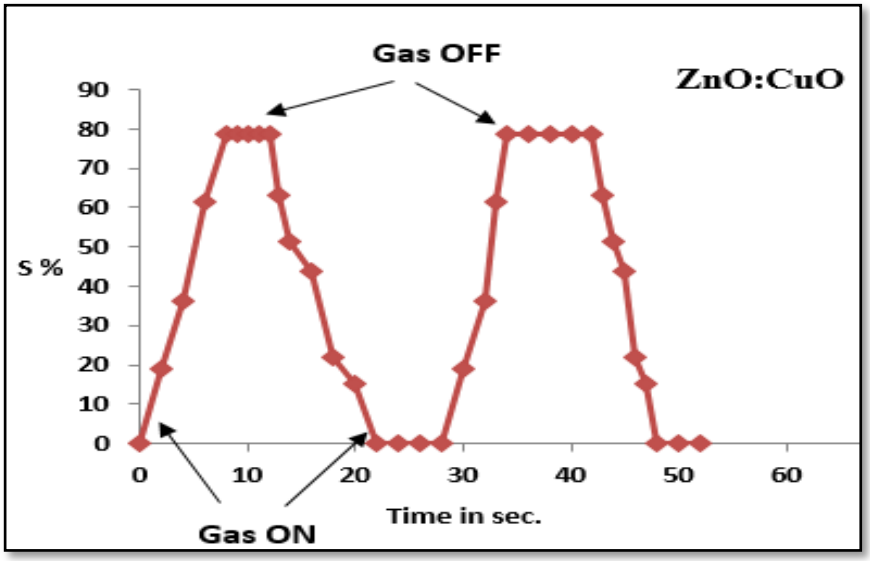

Figure 11 Response and recovery time of ZnO: CuO binary oxide thick film

From the time plot it is found that response time is 09 seconds whereas recovery time is 20 seconds to ZnO: CuO binary oxide thick film for H_2S gas at concentration 100 ppm and at 50 ^oC optimum temperature.

3.3.4 H_2S gas sensing mechanism for ZnO: CuO nano composite binary oxides thick film sample

ZnO is n-type semiconductors and CuO is a p-type semiconductor. Addition of ZnO into CuO makes ZnO: CuO nanocomposites binary oxide causes create p-n hetero junction that will promote high electrical resistance in the air [15, 16]. After exposure to H_2S gas, CuO is concerted into CuS phase shown in following reaction-

$CuO + H_2S = CuS + H_2O$

The effect of this reaction drastic increase electrical conductance result in decreases resistance of the film. The increase in percentage of ppm of Hydrogen gas sulfur atomic fraction increases which enhanced the sensitivity of the film because Cu decreases in these reaction and effect in change the resistance [17, 18].

References:

1. Anukunprasert, T., C. Saiwan, and Enrico Traversa. "The development of gas sensor for carbon monoxide monitoring using nanostructure of Nb–TiO2." *Science and Technology of Advanced Materials* 6.3-4 (2005): 359-363.
2. Eranna, G., et al. "Oxide materials for development of integrated gas sensors—a comprehensive review." *Critical Reviews in Solid State and Materials Sciences* 29.3-4 (2004): 111-188.
3. Balaguru, R. John Bosco, and B. G. Jeyaprakash. "Mimic of a gas sensor, metal oxide gas sensing mechanism, factors influencing the sensor performance and role of nanomaterials based gas sensors." *NPTEL–Electrical & Electronics Engineering–Semiconductor Nanodevices* (2004): 1-30.Sahm, T., et al. "Flame spray synthesis of tin dioxide nanoparticles for gas sensing." *Sensors and actuators B: Chemical* 98.2-3 (2004): 148-153.
4. Wang, Chengxiang, et al. "Metal oxide gas sensors: sensitivity and influencing factors." *sensors* 10.3 (2010): 2088-2106.
5. Dey, Ananya. "Semiconductor metal oxide gas sensors: A review." *Materials Science and Engineering: B* 229 (2018): 206-217.
6. Zhang, Jian, et al. "Metal-oxide-semiconductor based gas sensors: screening, preparation, and integration." *Physical Chemistry Chemical Physics* 19.9 (2017): 6313-6329.
7. Fine, George F., et al. "Metal oxide semi-conductor gas sensors in environmental monitoring." *sensors* 10.6 (2010): 5469-5502.
8. Bochenkov, V. E., and G. B. Sergeev. "Sensitivity, selectivity, and stability of gas-sensitive metal-oxide nanostructures." *Metal oxide nanostructures and their applications* 3 (2010): 31-52.
9. Bochenkov, V. E., and G. Bochenkov Sergeev. "Metal oxide nanostructures and their applications." *American Scientific Publishers* 3 (2010): 33.
10. Liu, Xiao, et al. "A survey on gas sensing technology." Sensors 12.7 (2012): 9635-9665.

11. Patil, Arun, et al. "Effect of Cr2O3 by Doping and Dipping On Gas Sensing Characteristics of ZnO Thick Films." *Journal of Electron Devices* 15 (2012): 1274-1281.

12. Tupe, U.J., Zambare, M.S., Patil, A.V. and Koli, P.B., 2020. The Binary Oxide NiO-CuO Nanocomposite Based Thick Film Sensor for the Acute Detection of Hydrogen Sulphide Gas Vapours. *Material Science Research India*, *17*(3), pp.260-269.

13. Li, Dan, et al. "Preparation and gas-sensing performances of ZnO/CuO rough nanotubular arrays for low-working temperature H2S detection." *Sensors and Actuators B: Chemical* 254 (2018): 834-841.

14. Kim, Jaehyun, Wooseok Kim, and Kijung Yong. "CuO/ZnO heterostructured nanorods: photochemical synthesis and the mechanism of H2S gas sensing." *The Journal of Physical Chemistry C* 116.29 (2012): 15682-15691.

15. Park, Sunghoon, et al. "Enhanced H2S gas sensing performance of networked CuO-ZnO composite nanoparticle sensor." *Materials Research Bulletin* 82 (2016): 130-135.

16. Wang, Xu, et al. "Low-temperature and highly sensitivity H2S gas sensor based on ZnO/CuO composite derived from bimetal metal-organic frameworks." *Ceramics International* 46.10 (2020): 15858-15866.

17. Nagarjuna, Yempati, and Yu-Jen Hsiao. "CuO/ZnO Heterojunction Nanostructured Sensor Prepared on MEMS Device for Enhanced H2S Gas Detection." *Journal of The Electrochemical Society* 168.6 (2021): 067521.

18. Vuong, Nguyen Minh, et al. "CuO-decorated ZnO hierarchical nanostructures as efficient and established sensing materials for H2S gas sensors." *Scientific reports* 6.1 (2016): 1-13.